Biosensors and Bioelectronics 120 (2018) 188–194

Contents lists available at ScienceDirect

Biosensors and Bioelectronics

journal homepage: www.elsevier.com/locate/bios

The electrical activity map of the human skin indicates strong differences between normal and diabetic individuals: A gateway to onset prevention

Constantin Ionescu-Tirgoviste[a,1], Paul A. Gagniuc[a,b,*,1], Elvira Gagniuc[c]

[a] National Institute of Diabetes, Nutrition and Metabolic Diseases "N.C. Paulescu", Bucharest, Romania
[b] Faculty of Engineering in Foreign Languages, Politehnica University of Bucharest, Romania
[c] University of Agronomic Sciences and Veterinary Medicine, Faculty of Veterinary Medicine Bucharest, Romania

ARTICLE INFO

Keywords:
Electrodermal activity
Skin
Patterns
Sensors
Human
Diabetes

ABSTRACT

The human skin is not only the largest organ, but also the most important candidate for novel non-invasive methods of investigation. Here we describe a large-scale prototype for determining the real-time distribution of the electrical activity from the surface of the human skin. A collection of 200 sensors have been placed across the entire trunk surface. The output of each sensor was remotely inserted into a 20 × 10 LED matrix for a parallel capture of the signals. Continuous observations of the electrical activity pattern were made above the LED matrix by a digital camera in an obscure environment. A total of 5.2 million measurements (25,920 maps) have been recorded as light intensities from the LED matrix and converted into percentages for evaluation. A total of 36 individuals were divided equally into two groups and subjected to a short glucose tolerance test for 1 h; one group with established *Type 2 Diabetes* (T2D) and the other group without diabetes. The electrical activity pattern and the average signal intensity of normal individuals (37% ± 8.1) and diabetic individuals (58% ± 7.8), showed a significant difference of 21%. The average signal intensity on the ventral side (VS) and dorsal side (DS) of the torso exhibited different behaviors in diabetics and non-diabetics. On average, diabetic individuals have shown an electrical activity of higher intensity on DS (DS = 60%, VS = 55%), while the normal group has shown a higher intensity on VS (DS = 36%, VS = 39%).

1. Introduction

Some organs of the human body often gained favor for more complex research because of their clear roles and immediate medical significance. In contrast, other organs with mixed and partly uncertain roles received less attention. The human skin is the *organum miraculos* as it has multiple roles and can be considered an important indicator for many disorders (Proksch et al., 2008; Si et al., 2015). More often than not, this organ has been brought to the forefront of diabetes for non-invasive diagnostic methods (Murphy-Chutorian et al., 2013; Duff et al., 2015; Nwabudike and Tatu, 2018). External chemical and biological fuels and the reuse of *self* molecular parts are the main energy components used by the body (Galgani and Ravussin, 2008; Hall et al., 2012). Environmental parameters force the human body to use unique behavioral patterns for energy intake (Carreiro et al., 2016). Thus, the manner in which these resources are used by the body over time dictate the behavior of the metabolic machine and the impact of this behavior on homeostasis (Han et al., 2015; Savir et al., 2017). For a large proportion of the human population, certain mechanisms in the metabolic chain are only partially adapted to the variability of the environmental parameters due to genetic susceptibility and inheritance or *de novo* somatic mutations (Karaderi et al., 2015; De Silva and Frayling, 2010). A low adaptation to a broad range of environmental conditions implies a predisposition of the body to certain diseases, which are triggering only under specific conditions (Ionescu-Tîrgovişte et al., 2015). More often, particular deviations of the metabolic behavior can trigger diseases such as type 2 diabetes (Galgani and Ravussin, 2008; Hall et al., 2012). A non-invasive method to probe the metabolic behavior is represented by the electrical activity that can be sampled from the surface of the skin (Nuccitelli et al., 2011; Thorell et al., 2013). However, the lack of useful imaging methods for in vivo studies of metabolic diseases would be the main rationale behind our current investigation. Diabetes

Abbreviations: BMI, Body Mass Index; ECG, Electrocardiograph; EDA, Electrodermal Activity; EEG, Electroencephalograph; HbA1C, Glycated hemoglobin; LED, Light-Emitting Diode; T2D, Type 2 Diabetes; VSL, Vertical Sensor Lines

* Corresponding author at: National Institute of Diabetes, Nutrition and Metabolic Diseases "N.C. Paulescu", Bucharest, Romania.
E-mail address: paul_gagniuc@acad.ro (P.A. Gagniuc).

[1] Co-first authors.

https://doi.org/10.1016/j.bios.2018.08.057
Received 26 January 2018; Received in revised form 17 August 2018; Accepted 23 August 2018
Available online 25 August 2018
0956-5663/

implications on the global metabolic status of the body served as our initial hypothesis for a detailed exploration of the electrical activity of the skin. Ions from individual cells and moving fluids are the origin of the electrical signals (potentials and currents) generated by the human body. Sodium (Na^+) and potassium (K^+) are the most important examples of monovalent cations with a single positive charge or calcium (Ca^{2+}), which is a divalent cation that carries a double positive charge. Thus, the electrical activity represents the change in electric current produced by the sum of an electrical potential difference across a specialized tissue, organ or cell system. By our knowledge, a high resolution of sensors for macro-detection of electrical fluctuations of the skin has not been used in past investigations. Here we propose a novel prototype for direct observations on the subtle metabolic processes through high resolution electrical activity patterns. In our approach the electrical activity is observed through a large collection of 200 sensors located over the surface of the trunk. Thus, a high resolution of the electrical activity generated by the trunk is obtained and analyzed comparatively between normal and diabetic individuals.

2. Materials and methods

In order to make direct observations on the subtle metabolic processes in normal and disease conditions, we built a prototype measuring device called „Vesta" (Gagniuc et al., 2018). The system was composed of a coat equipped with 200 sensors and a signal recording box that was able to transfer the data to a computer in real-time. Changes in the electrical signal patterns over time during a short glucose tolerance test, have been the main objective of this experiment (Fig. 1).

2.1. Sensor internals & organization

Eight electronic parts have been attached to a printed circuit board (PCB) for each sensor: three BC546B general-purpose NPN bipolar junction transistors (Q1,Q2, and Q3) arranged in a Darlington triplet, an electrode wire (L = 2 cm,d = 0.5 mm), three resistors, R1(1 MΩ), R2 (100 kΩ), R3 (100 Ω), and L1, a *Light-Emitting Diode* (LED) that resides outside the PCB of the sensor (Fig. 1a). A coat without sleeves that molds over the human torso was chosen in order to allow the skin an optimal exchange with the environment (Supplementary material 1). 200 sensors were arranged and sewn on the outer part of the vest in 16 *Vertical Sensor Lines* (VSL). The electrode of each sensor penetrated through the vest material and established a physical contact with *stratum corneum*. The VSL consisted of 11–13 sensors arranged linearly on the vest, in accordance with the anatomy of the human torso. The ventral and dorsal side of the torso were covered by 8 VSL each. Thus, the torso VSL coverage was made between T1 and L4 or L5 vertebrae. Sensor labeling was made by using the number associated with a VSL, followed by the sensor number along the VSL (Fig. 1b,c).

Supplementary material related to this article can be found online at doi:10.1016/j.bios.2018.08.057.

2.2. LED matrix organization and signal encoding

The 200 LEDs have been positioned outside of the vest environment by using insulated copper wires. The LEDs of the sensors have been arranged on a PCB into a 20 × 10 LED matrix of 12 × 6 cm in size. 100 LEDs of VSL from the dorsal side of the torso were encoded (positioned) on the first half of the LED matrix (left side) whereas the 100 LEDs of VSL from the ventral side have been encoded on the second half (Fig. 1d). The encoding was made in a zigzag pattern starting from the right to the left, for both sides of the LED matrix.

2.3. The electric diagram of the vest

The main electrode and the positive/negative terminals represented the input of each sensor (S_1, S_2 … Sn, where n = 200). Thus, VSL were powered in parallel using a DC power supply (7.5 V). The electrode had the task of collecting and transmitting the local biological signal to the base of the Q1 transistor for further amplification. The output of each sensor was represented by the signal from the collector of the Q3 transistor and it was connected remotely to the corresponding LED anode by an insulated copper wire. The positive terminal (+) of the DC power supply was connected to the VSL and to the cathode of each LED in the matrix. The negative terminal (-) of the DC power supply was grounded and also connected to the emiter of each Q3 transistor from the VSL. The connection between the vest and the signal recording box was made through a total of 232 insulated copper wires. Of which, 200 wires bring the amplified signal from each sensor to the LED matrix and 32 wires feed the VSL.

2.4. The black box & data acquisition

In the absence of ambient light, a digital camera (320 × 240 pixels) was used as a light detector. A digital camera supported by a duralumin skeleton, was targeted at 15 cm above the LED matrix inside an opaque box (Fig. 1e). A dedicated opensource software was developed for the video camera and used to retrieve the images of the LED matrix at discrete time intervals. The optimal setting for our experiment was established at 60 min with an interval of 5 s, which resulted in a constant series of 720 images/subject (25920 images for the entire experiment). These images were stored on a computer for further analysis.

2.5. Presentation of groups

A total of 36 individuals were divided into two groups: the normal group (-); composed of 5 normal females (F-) and 13 normal males (M-) and a diabetic group (+); consisting of 8 diabetic females (F+) and 10 diabetic males (M+). *Glycated hemoglobin* (HbA1C) values and prior diagnosis of T2D metabolic syndrome were the main parameters for inclusion into the group. The diabetic group included individuals with HbA1C values above the 6.5% threshold whereas individuals with values below 5.9% were associated with the normal group. On average, individuals belonging to the diabetic group (+) showed a HbA1C value of 7.82 ± 0.7 (F(+) = 7.88 ± 0.7 and M(+) = 7.77 ± 0.73), and the normal group (-) showed a HbA1C value of 5.45 ± 0.25 (F (-) = 5.46 ± 0.27 and M(-) = 5.44 ± 0.26). The *Body Mass Index* (BMI) was calculated in order to observe the balance between female and male groups (Supplementary material 2). Diabetic females F(+) showed an average age of 66 ± 8.9 years and a BMI of 32.41 (*height* = 156 ± 9, *weight* = 79 ± 15), while diabetic males M(+) showed an average age of 63.9 ± 8.8 years and a BMI of 29.87 (h = 173.3 ± 7.6, w = 89.7 ± 17.4). In the normal group, females F (-) showed an average age of 52.6 ± 16.14 years and a BMI of 30.71 (h = 165 ± 10.2, w = 83.6 ± 38.3), while normal males M(-) showed an average age of 37.38 ± 16.73 years and a BMI of 26.51 (h = 181.46 ± 9.48, w = 87.31 ± 11.59).

2.6. Experiment design

Volunteer patients participated in the experiment in a dry fasting state. Each experiment was conducted in the morning (3 subjects/day). To avoid an increase in the apparent temperature of the body, constant temperature (25 °C) and relative humidity (40%) have been preserved around the experimental setup. During the experiments, the subjects had to wear the vest and sit comfortably and immobile for 1 h on a chair without a backrest. In order to closely observe the metabolic response, two oral doses of 37 g glucose have been administered to the subjects (Fig. 1f). The first dose was administered after 15 min and the second dose after 30 min (75 g in total). Each participant was carefully monitored for blood glucose levels in *milligrams per deciliter* (mg/dL) at 15-

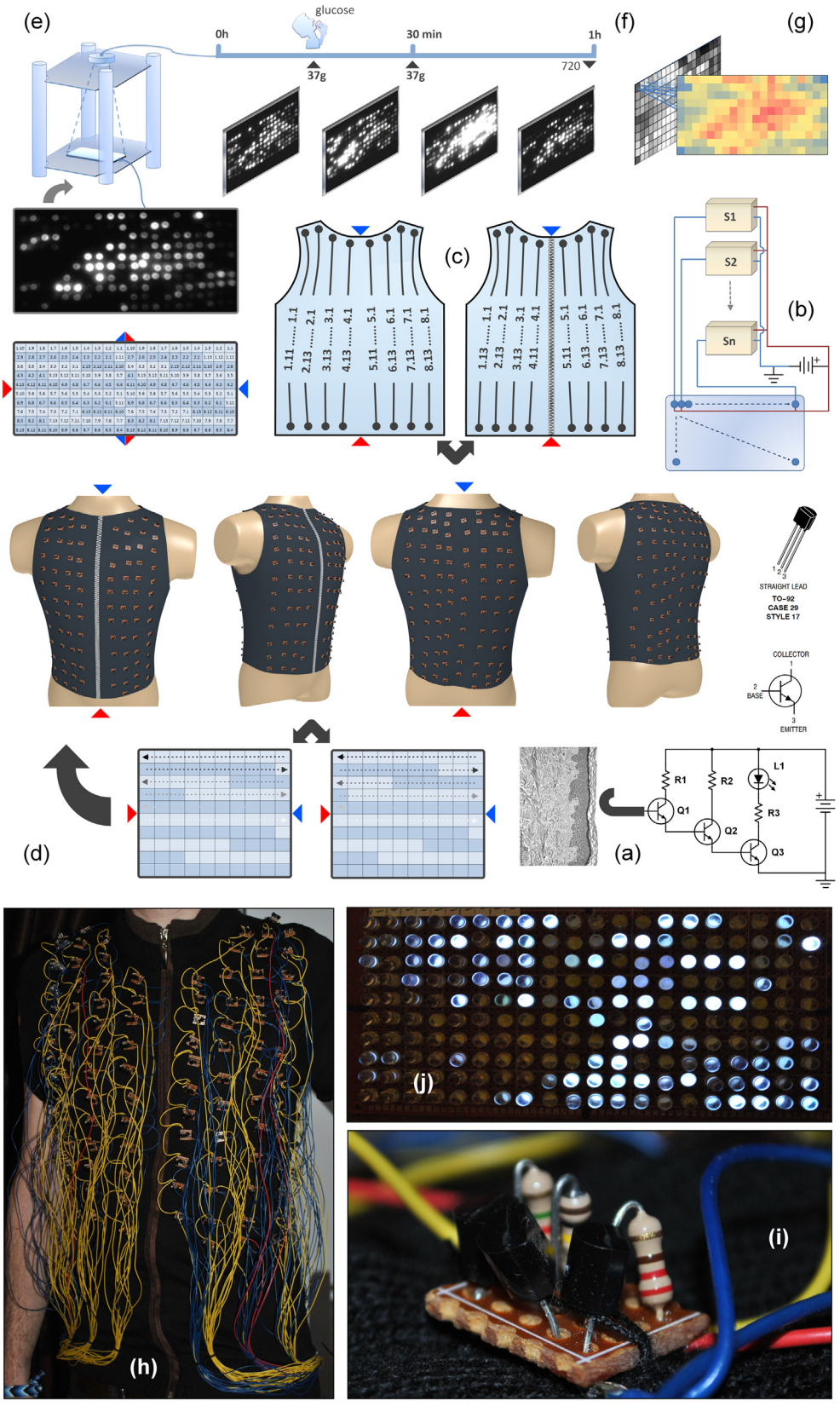

Fig. 1. The general diagram of the experiment. (a) The sensor diagram and a section through the epidermal layers. The electronic parts: Q1,Q2, Q3 (BC546B), R1(1 MΩ), R2 (100 kΩ), R3 (100 Ω). (b) The overall electrical diagram of the system. The dark yellow boxes (S_1 … S_n) represent the sensors, where $n = 200$. The negative terminal (-) of the DC power supply is represented by the blue lines, while the positive terminal (+) is represented by dark red lines. The light blue rectangle represents the LED matrix. The blue circles inside the light blue rectangle represent the LEDs. The lines that connect these circles to the dark yellow boxes signify the connection between the collector of the Q3 transistor (through the R3 resistor) and the cathode of the LED. (c) The organization of the *vertical sensor lines(VSL)* on the ventral (right) and dorsal (left) surface of the vest. The red triangle represents the bottom of the vest and the blue triangle represents the top of the vest. On each surface, the *VSL* are labeled from 1 to 8, starting from the left. The sensors on the *VSL* are labeled from 1 to 11 or 13, starting from the bottom to the top of the vest. (d) The organization of *VSL* on the LED matrix. The LEDs that correspond to the *VSL* are arranged in a zig zag pattern starting from the right. (e) A video camera targeted on the LED matrix in an obscure environment depicts *the black box*. (f) A total of 720 images of the LED matrix are recorded over a period of 1 h. During this interval, two oral doses of 37 g glucose are administered to the subject in order to observe the metabolic response. (g) Extraction and analysis of the data. (h) The ventral side of the electrodermal vest. The image shows 100 sensors arranged in 8 VSL attached to the vest. The *VSL* from the ventral side are connected to 16 power cables (2 power cables for each *VSL*) and 100 signal cables tightly arranged in the immediate vicinity of the base of the vest, (j) The LED matrix powered by the DC power supply at 7.5 V. (For interpretation of the references to color in this figure legend, the reader is referred to the web version of this article.).

min intervals, namely: t_0 (0 min), t_1 (15 min), t_2 (30 min), t_3 (45 min) and t_4 (60 min). Before each experiment, the electrodes of the sensors were individually disinfected and tested.

2.7. Calibration & analysis

The LEDs coordinates from the 320 × 240 images were stored in vector format for further use in the extraction of light intensities: $v^{(n)} = [x,y]$, where n represents the index of the LED in the matrix, and the $[x,y]$ components represent the coordinates of the brightest pixel on the image for that particular LED. The collected pixel values were converted into percentages, where pure black was 0% and pure white was 100%. In this manner, electrical activity heatmaps were built and analyzed (Fig. 1g). More technical details can be found in Fig. 1h-j.

3. Results and discussion

The torso was used to assess the electrical characteristics of the skin under the influence of metabolic stimuli. In our case, the metabolic stimuli consisted of oral glucose doses taken by the participants at well-

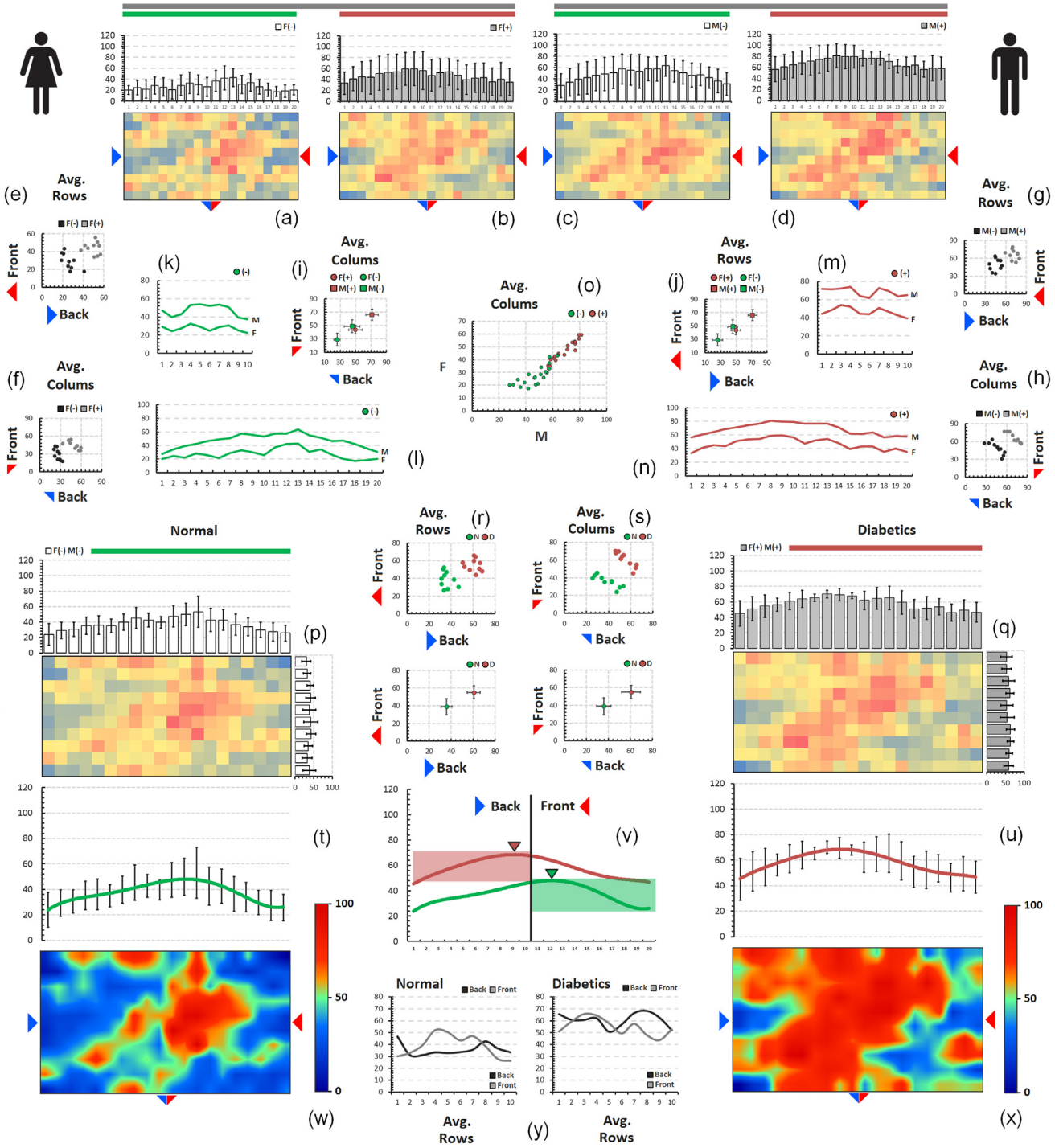

(caption on next page)

Fig. 2. The average of the LEDs by group and gender. (a) Heatmap representing the average across all LED matrices of normal females (F-), (b) diabetic females F(+), (c) normal males M(-), (d) diabetic males M(+). The chart above each heatmap (panels a-d) shows the average of the signals on the columns of the heatmap matrix. Colors represent signal intensities from 0% (blue) to 100% (red). The green color is associated with normal individuals whereas the burgundy color is associated with diabetic individuals. The blue triangles represent the dorsal side and red triangles represent the ventral side. (e) The average values from the rows of the first half of the matrix (back side) plotted against the average values from the rows of the second half of the matrix (front side). (f) The average values of the columns from the first half of the matrix (back side) plotted against the average values of the columns from the second half of the matrix (front side). In both e and f panels, the gray bullets represent the matrix from F(+) whereas black bullets represent the matrix from F(-). (g) The average values of the rows from the first half of the matrix (back side) plotted against the average values of the rows from the second half of the matrix (front side) in M(-) and M(+). (h) The average values from the columns of the first half of the matrix (back side) plotted against the average values of the columns from the second half of the matrix (front side) in M(-) and M(+). In both g and h panels, the gray bullets represent the matrix from M(+) whereas black bullets represent the matrix from M(-). (i) The distribution of the average signal from the back side rows plotted against the average signal from the front side rows for each of the four matrices (F-,F+,M-,M+). (j) The distribution of the average signal from the back side columns plotted against the average signal from the front side columns for each of the four matrices (a-d). (k) The average signal from the rows of matrix M (-) and F(-). (l) The average signal from the columns of matrix M(-) and F(-). (m) The average signal from the rows of matrix M(+) and F(+). (n) The average signal from the columns of matrix M(+) and F(+). (o) distribution of normal (F-,M-) and diabetic individuals (F+, M+). Green dots represent the average signal from columns of F(-) against the average signal from columns of M(-). Reddish dots represent the average signal from columns of F(+) against the average signal from columns of M(+). (p) The average matrix between F(-) and M(-). Represents the global pattern of normal individuals. (q) The average matrix between F(+) and M (+). Represents the global pattern of diabetic individuals. (r) The average values from the rows of the first half of the global matrix (back side) plotted against the average values from the rows of the second half of the global matrix (front side). The center of each cluster is shown below this graph. (t) The trend of the average signal on the columns of the global matrix from panel (p). (s) The average values from the rows of the first half of the diabetic global matrix (back side) plotted against the average values from the rows of the second half of the diabetic global matrix (front side). The center of each cluster is shown below this graph. (w) Heatmap of the electrical activity derived from the global matrix of panel (p). (u) The trend of the average signal on the columns of the global matrix. (v) Comparison between the average signals on the columns of the normal matrix from panel (p) and diabetic matrix from panel (q). (x) Heatmap of the electrical activity derived from the global matrix of panel (q). (y) The average signals on the rows of the back side against the average signals on the rows of the front side; in normal (left) and diabetic individuals (right). (For interpretation of the references to color in this figure legend, the reader is referred to the web version of this article.).

defined time intervals throughout each experiment. As expected, the glycemic range was higher in the diabetic group (max = 489 mg/dL, min = 111 mg/dL) compared to the normal group (max = 272 mg/dL, min = 89 mg/dL). High glycemic values recorded in both groups are explained by a short tolerance test (75 g of glucose/1 h).

3.1. Electrical activity in normal vs. diabetic individuals

The average signal intensity of normal (37% ± 8.1) and diabetic individuals (58% ± 7.8), showed a categorical difference of 21% (Supplementary material 3). The average signal intensity on the front side (ventral) and back side (dorsal) of the torso indicated different behaviors in diabetics and non-diabetics. On average, diabetic individuals showed an electrical activity of higher intensity on the back side (front = 55%, back =; 60%), while the normal group showed a higher intensity on the front side of the torso (front = 39%, back = 36%).

3.2. Gender differences within/between groups

Within groups, gender differences have been observed in regard to the average electrical activity. In the normal group, F(-) showed an average signal value of 27% ± 8 and M (-) showed a mean value of 47% ± 10 (20% difference). In the diabetic group, the percentage difference between genders was of 22% (M (+) = 69% ± 9, F (+) = 47 ± 8). Between males of the two groups (M+ vs. M-), there was a difference of 22% in the average signal intensity. Also, among the females of the two groups (F + vs. F-) there was a 19% difference in the average signal intensity.

3.3. Average signal activity on the ventral and dorsal part of the torso

3.3.1. Back vs. front in males

Diabetic males M (+) have shown an average signal intensity of 71% ± 6 on the back side and 66% ± 8 on the front side of the vest. In the case of diabetic males the difference in the average signal intensity between the back and the front of the vest was ~5%. In the normal group, males showed a balanced signal intensity between the front (49% ± 10) and the back (46% ± 6) of the vest. The difference between the front and the back of the vest in normal males was only of 3%. A comparison between males of the two groups (front; M+ vs. M-), regarding the average signal intensity on the front side of the vest showed a difference of 17% while on the back side it showed a difference of 26%.

3.3.2. Back vs. front in females

Diabetic females F(+) have revealed an average signal intensity of 50% ± 6 on the back side and 44% ± 7 on the front side of the vest. In the case of diabetic females the difference in the average signal intensity between the back and the front of the vest was ~6%. In the normal group, females showed a balanced signal intensity between the front (29% ± 9) and the back (26% ± 7) of the vest. The difference between the front and the back of the vest in normal females was only of 3%. A comparison between the females of the two groups (front; F+ vs. F-) on the average signal intensity from the front side of the vest showed a difference of 15% while on the back side it showed a difference of 24%.

3.4. The electric activity distribution by gender

A total of 25,920 images of the LED matrix (5.2 million measurements) have been used to compile 4 global matrices, representing the average electrical activity of the torso for each gender of the two groups (Fig. 2a-d). The mean values of the rows and columns of these matrices were considered. A distribution of ventral vs. dorsal average electrical signals showed separate clusters for the males of the two groups and for the females of the two groups (Fig. 2e-j). The distribution of the average values of each row or column of the matrix has shown particular trends and intensity differences between males and females of the normal group (Fig. 2k,l). A similar gender difference was also observed in the diabetic group (Fig. 2m,n). Moreover, a distribution of females vs. males of each group also presented separate clusters (Fig. 2o).

3.5. The electrical activity distribution in normal vs. diabetic individuals

A global matrix of the electrical activity was compiled for each group (Fig. 2p,q). The averages on the rows and columns of these two global matrices have been considered. Ventral vs. dorsal comparisons of the average values of the electrical signals, showed separate clusters in normal and diabetic subjects (Fig. 2r,s). The averages of the columns of each matrix were plotted separately for each group and distinctive trends have been observed (Fig. 2t,u). Next, the two distributions were overlapped (Fig. 2v). Thus, Fig. 2v shows a higher electrical activity on the back side of the vest in diabetics and a higher activity on the front of

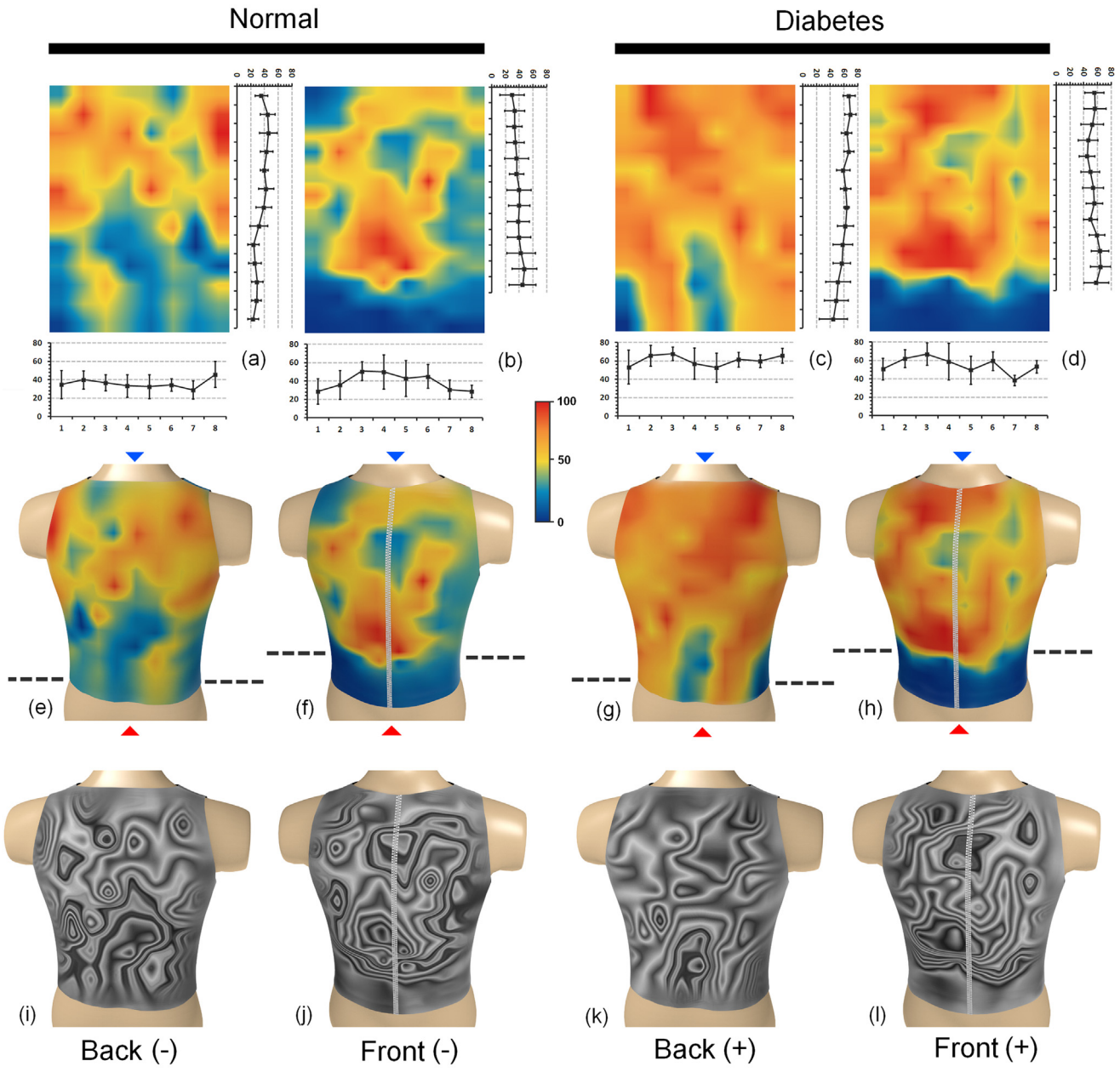

Fig. 3. The average 2D-3D topographic map of the torso electrical activity. (a) dorsal (back side) heatmap of the average electrical activity in normal individuals, (b) ventral (front side) heatmap of the average electrical activity in normal individuals, (c) dorsal heatmap of the average electrical activity in diabetic individuals, (d) ventral (front side) heatmap of the average electrical activity in diabetic individuals. The red color represents the maximum average intensity whereas the blue color is the minimum mean intensity. The charts at the bottom and right of each heatmap represent the column averages and the line averages. (e) dorsal heatmap of normal individuals and (f) ventral heatmap of normal individuals molded on a 3D torso model. (g) dorsal heatmap of diabetic individuals and (h) ventral heatmap of diabetic individuals molded on a 3D torso model. The interrupted lines indicate the lower bound of the sensors on each face. The blue and red triangles correspond to the configuration shown in the first figure from materials and methods. Their meaning is to perceive the correspondence between the sensors and the matrix. (i) dorsal topographic map in normal individuals, (j) ventral topographic map in normal individuals, (k) dorsal topographic map in diabetic individuals, (l) ventral topographic map in diabetic individuals. (For interpretation of the references to color in this figure legend, the reader is referred to the web version of this article.).

the vest in normal subjects. To increase the details of the average matrix of diabetic and normal individuals, a bilinear interpolation filter was used (Fig. 2w,x).

3.6. Consistent signatures and trend features

In our approach we tried to give more emphasis to the shape and trend of the signals than to their global levels. The average signals on the rows of the each matrix have proven to be more discriminatory than those on the columns (Fig. 2y). The average signals on the back and front rows showed characteristic superimposed shapes for diabetics and normal individuals regardless of the global intensity of the signals (Fig. 2y).

3.7. Three-dimensional maps of the electrical activity of the skin

The encoded matrices of the two groups were decoded in order to observe the true shapes taken by the average electrical activity

generated by the torso (Fig. 3a-d). The transposition of the first half of the encoded matrix revealed the real distribution of the electrical activity from the dorsal side of the torso (Supplementary material 4 and 5).

In contrast, the transposition of the second half of the encoded matrix revealed the distribution from the ventral side of the torso. A bilinear interpolation filter has been used to increase the resolution of the sensors (Fig. 3a-d). Thus, the decoded heatmaps were molded onto a three-dimensional mesh for a correct representation of reality (Fig. 3e-h). Decoded maps show an average electrical activity more pronounced and diffuse in diabetics compared to non-diabetics (Fig. 3e-h and Supplementary material 6 and 7).

Supplementary material related to this article can be found online at doi:10.1016/j.bios.2018.08.057.

3.8. The past, present and the future

In the past, the most commonly used in vivo approaches have involved glycated proteins or individual electrodes to measure the *Electrodermal Activity* (EDA) (Beisswenger et al., 2001). Historically, the EDA field has led to critical equipment such as the *Electrocardiograph* (ECG) or the *Electroencephalograph* (EEG) (Waller, 1887; Hurst, 1998). More recent additional phenomena within EDA field, such as resistance, potential, impedance, and admittance, have brought new results that have amplified the unknowns in the electrical complexity of the body (Tronstad et al., 2013, 2008; Woo et al., 1992). In physiology, frequent approaches in skin research and disease manifestation have involved optical or thermal characterizations of the skin properties (Pfefer et al., 2009). However, to our knowledge, a large-scale study of the electrical activity of the skin has never been conducted in this manner. About 70% of patients with diabetes are affected by hypertension (Lago et al., 2007). Before the onset of diabetes many tissues of the human body undergo subtle changes that are usually unnoticed by medical practitioners. Here, these changes are reflected in a comparative manner by the electrical activity (Ionescu-Tirgoviste et al., 2018). The contour lines of the electrical activity of the skin have been considered for a topographic map of the two groups (Fig. 3i-l). This approach indicated a higher definition and complexity (low entropy) of the electric activity from normal individuals compared to diabetic individuals. The electrical activity patterns open up future possibilities for type 2 diabetes prediction and high potential for risk assessment in therapeutic interventions prior to the onset of the disease.

4. Conclusions and perspectives

A novel large-scale prototype was designed and built to detect the real-time 2D and 3D distribution of the electrical activity from the surface of the human torso. A diabetic and a normal group have been studied in connection with the intensity and distribution of the electrical activity. Different and characteristic signatures have been observed. Our results show an average signal intensity difference between diabetics and normal individuals of 21%. Additional ongoing work involves an increase in the number of subjects and the number of sensors used on the human torso. This will enable us to increase the resolution of the electrical activity and the power of discrimination between different metabolic diseases.

Acknowledgements

The authors declare no competing financial interests. Dr. Paul A. Gagniuc would like to acknowledge his former students from Politehnica University of Bucharest: a). Ing. Serban Radu Gabriel, for the astonishing 3D animations and the 3D model of the human torso. b) Ing. Stefan-Alexandru Paun, Ing. Alexandru-Ioan Berbescu and Ing. Anas Semreen for active participation in the implementation of the sensors and strict adherence to the design protocols. c). Ing. Bogdan Taloi, for the time spent on TensorFlow adaptation to the experimental data derived from the “Vest” prototype. We thank to all 36 participants in the study for their patience. All experiments were performed in accordance with relevant guidelines and regulations. The methods were carried out in accordance with the approved guidelines. Prior to the experiment, volunteers have been asked in advance if they have a pacemaker installed. All subjects have signed an informed consent. All experimental protocols were approved by the Ethical Committee of “NC Paulescu” National Institute of Diabetes. As the experiments unfolded the patients were carefully monitored by a physician and a dose of injectable insulin has always been available. However, such an intervention was not necessary.

Author contributions

PAG and CIT conceived of the study and participated in its design and coordination. PAG designed and implemented the prototype. PAG invented the parallel signal acquisition system. PAG created the algorithms and the software used in the analysis. CIT composed the normal and diabetic groups. CIT, EG and PAG have conducted the experiments. PAG, CIT, EG analyzed the data. EG, CIT verified the data. PAG designed the figures and tables according to the main results. PAG, CIT and EG wrote the paper. All authors have verified the accuracy of the data. All authors discussed the results and commented on the manuscript.

Appendix A. Supplementary material

Supplementary data associated with this article can be found in the online version at doi:10.1016/j.bios.2018.08.057.

References

Beisswenger, P.J., Szwergold, B.S., Yeo, K.T., 2001. Clin. Lab. Med. 21 (1), 53–78.
Carreiro, A.L., Dhillon, J., Gordon, S., Jacobs, A.G., Higgins, K.A., McArthur, B.M., Redan, B.W., Rivera, R.L., Schmidt, L.R., Mattes, R.D., 2016. Annu. Rev. Nutr. 36, 73–103.
De Silva, N.M., Frayling, T.M., 2010. Curr. Opin. Lipidol. 21 (1), 44–50.
Duff, M., Demidova, O., Blackburn, S., Shubrook, J., 2015. Clin. Diabetes 33 (1), 40–48.
Gagniuc, P.A., Ionescu-Tirgoviste, C., Gagniuc, E., 2018. Methods X (In press).
Galgani, J., Ravussin, E., 2008. Int. J. Obes. (Lond.). 32 (Suppl. 7), S109–S119.
Hall, K.D., Heymsfield, S.B., Kemnitz, J.W., Klein, S., Schoeller, D.A., Speakman, J.R., 2012. Am. J. Clin. Nutr. 95 (4), 989–994.
Han, W., Chuang, K.H., Chang, Y.T., Olivo, M., Velan, S.S., Bhakoo, K., Townsend, D., Radda, G.K., 2015. Diabetes Metab. Res. Rev. 31 (1), 14–35.
Hurst, J.W., 1998. Circulation 98 (18), 1937–1942.
Ionescu-Tirgoviste, C., Gagniuc, P.A., Gagniuc, E., 2018. Data in Brief (In press).
Ionescu-Tîrgovişte, C., Gagniuc, P.A., Guja, C., 2015. PLoS One 10 (9), e0137950.
Karaderi, T., Drong, A.W., Lindgren, C.M., 2015. Curr. Diab. Rep. 15, 83.
Lago, R.M., Singh, P.P., Nesto, R.W., 2007. Nat. Clin. Pract. Endocrinol. Metab. 3 (10), 667.
Murphy-Chutorian, B., Han, G., Cohen, S.R., 2013. Endocrinol. Metab. Clin. North. Am. 42 (4), 869–898.
Nuccitelli, R., Nuccitelli, P., Li, C., Narsing, S., Pariser, D.M., Lui, K., 2011. Wound Repair Regen. 19 (5), 645–655.
Nwabudike, L.C., Tatu, A.L., 2018. J. Eur. Acad. Dermatol. Venereol. https://doi.org/10.1111/jdv.15084.
Pfefer, T.J., Mehrabi, A., James, R., Landry, R., Weininger, S., Chang, I., Kaufman, D., Miller, S., 2009. Phys. Med. Biol. 54 (22), 6867–6880.
Proksch, E., Brandner, J.M., Jensen, J.M., 2008. Exp. Dermatol. 17 (12), 1063–1072.
Savir, Y., Martynov, A., Springer, M., 2017. PLoS Comput. Biol. 13 (4), e1005458.
Si, J., Lee, S., Park, J.M., Sung, J., Ko, G., 2015. BMC Genom. 16, 992.
Thorell, L.H., Wolfersdorf, M., Straub, R., Steyer, J., Hodgkinson, S., Kaschka, W.P., Jandl, M., 2013. J. Psychiatr. Res. 47 (12), 1925–1931.
Tronstad, C., Kalvøy, H., Grimnes, S., Martinsen, Ø.G., 2013. Psychophysiology 50 (11), 1070–1078.
Tronstad, C., Martinsen, O.G., Grimnes, S., 2008. Conf. Proc. IEEE Eng. Med. Biol. Soc. 2008, 2373–2376.
Waller, A.D., 1887. J. Physiol. 8 (5), 229–234.
Woo, E.J., Hua, P., Webster, J.G., Tompkins, W.J., Pallás-Areny, R., 1992. Med. Biol. Eng. Comput. 30 (1), 97–102.